

## THE FORMATION OF BINARY-VORTEX STREET BEHIND TWO CIRCULAR CILINDERS ARRANGED IN TANDEM

Paulo Guimarães de Moraes, pauloguimor@yahoo.com.br

Luiz Antonio Alcântara Pereira, luizantp@unifei.edu.br

Institute of Mechanical Engineering, Federal University of Itajubá, CP 50, Av. BPS, 1303, CEP. 37500-903, Itajuba, MG, Brazil

Miguel Hiroo Hirata, hirata@fat.uerj.br

State University of Rio de Janeiro, FAT-UERJ, Resende, Rio de Janeiro, Brazil

**Abstract.** Numerical investigations on the characteristics of the flow around a pair of immovable circular cylinders arranged in tandem were carried out. A purely Lagrangian Vortex Method was associated with a Poisson equation for the pressure to calculate global as well as local quantities at a supercritical Reynolds number ( $Re=65,000$ ). The dominant vortex shedding frequencies in the wake of two cylinders were measured simultaneously using two fixed points placed behind each cylinder. A discontinuous jump on drag coefficient and Strouhal number was identified at a critical centre-to-centre distance between the cylinders; this behavior was found due to bi-stable nature of the gap flow. When the distance was larger than the critical spacing, the flow pattern was referred as co-shedding type, with both cylinders shedding vortices. For some pitch ratios there may be synchronization between the vortex shedding process and the vortex streets of the upstream and downstream cylinders, and the possible formation of a binary-vortex street behind downstream cylinder. A primary focus on the formation of binary-vortex street was analyzed in this study.

**Keywords:** flow around two cylinders, in tandem, dominant vortex frequencies, wake interference, vortex method.

### 1. INTRODUCTION

The effects of the interference between bodies in close proximity to one another can change fundamental aspects of the flow, such as fluid forces, separation point, vortex shedding frequency and dynamics of vortices. In the case of bluff bodies, the fluid flow around circular-cylindrical structures have received much attention of researchers as a result of its relevance in a variety of industrial settings: offshore platforms, heat-exchangers, nuclear power plants, buildings, chimneys, and so on. In the literature, the type of interference between two cylinders configurations is called flow interference (Zdravkovich, 1987). The wake interference is a particular type of flow interference, in which one cylinder is partially or completely immersed in the wake of another cylinder. A second type of interference was classified as proximity interference, in which both cylinders are located close to one another, but neither is immersed in the wake of the other. The flow around pairs of immovable circular cylinders has been the starting point to understand these ones basic types of interference. There are several comprehensive reviews of the flow around two circular cylinders in different arrangements. In particular, Zdravkovich (1977) and Sumner (2010) presented approaches to understanding the fluid behaviour. Three categories of arrangements can be classified based on the angles ( $\alpha$ ) of the center connection line of the cylinders relative to the main stream direction: in tandem ( $\alpha=0^\circ$ ), side by side ( $\alpha=90^\circ$ ) and staggered ( $0^\circ < \alpha < 90^\circ$ ).

In this work, a particular type of arrangement has been investigated: two immovable circular cylinders of equal diameter arranged in-line and parallel to the main stream at a high Reynolds number. The flow patterns are sensitive to both Reynolds number ( $Re$ ) and the centre-to-centre longitudinal pitch ratio ( $g/d$ ), being  $d$  the cylinder diameter. The pioneer studies of the tandem arrangement were presented by Igarashi (1981, 1984), in which were identified eight different flow patterns for two tandem circular cylinders. In recent numerical works, Carmo *et al.* (2010a, 2010b) classified the flow around two circular cylinders at low Reynolds numbers ( $Re=50-500$ ) in three main flow patterns: (i) SG (symmetric in the gap) observed at  $g/d=1.5$ ; (ii) AG (alternating in the gap) observed at  $g/d=1.8$  and  $2.3$  and (iii) WG (wake in the gap) observed at  $g/d=5$ . Their classification scheme was similar to that given by Xu and Zhou (2004) and Zhou and Yiu (2006). A Lagrangian mesh-free Vortex Method (Moraes, 2011) is used here to simulate the two-dimensional, time dependent viscous incompressible flow around two circular cylinders in tandem arrangement.

### 2. NUMERICAL METHOD

Consider the viscous flow around two circular cylinders in tandem arrangement as shown in “Fig. 1”. The boundary  $S$  of the fluid domain is defined as  $S=S_1 \cup S_2 \cup S_\infty$ , being  $S_1$  and  $S_2$  the circular cylinder surfaces upstream and downstream, respectively and  $S_\infty$  the far away boundary (which can be viewed as  $r = \sqrt{x^2 + y^2} \rightarrow \infty$ ). In order to avoid possible interference, the two fixed points were used to determine vortex shedding frequencies,  $P(x,y)$  and  $Q(x,y)$ , respectively in “Fig. 1”. Xu and Zhou (2004) used similar schematic arrangement for hot-wire measurements.

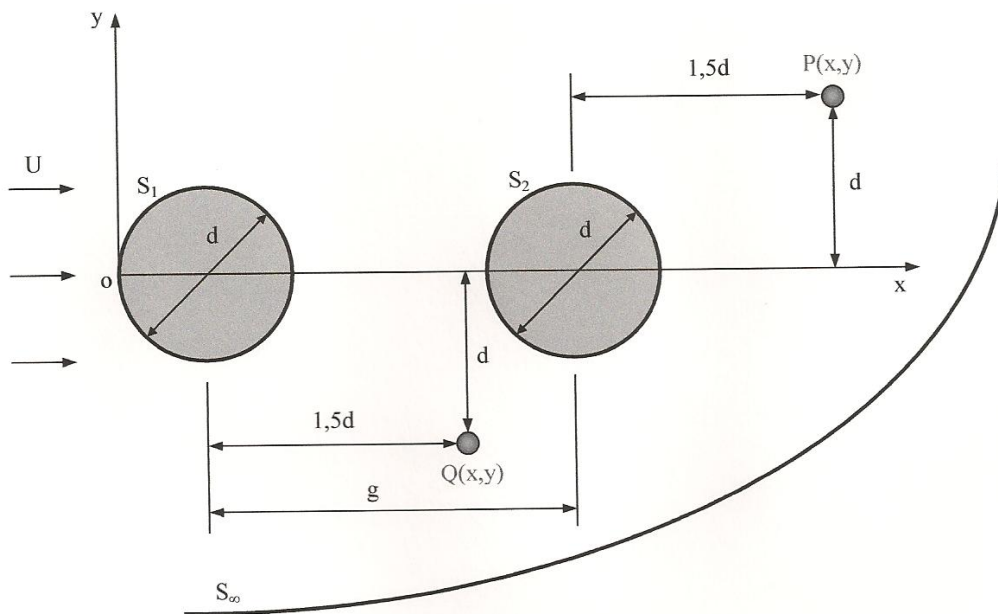


Figure 1. Schematic arrangement of two in-line cylinders.

The dynamics of the fluid motion is studied in a more convenient way taking the curl of the Navier-Stokes equations to obtain the vorticity equation

$$\frac{\partial \omega}{\partial t} + \mathbf{u} \cdot \nabla \omega = \frac{1}{\text{Re}} \nabla^2 \omega \quad (1)$$

where  $\omega(\mathbf{x}, t) = \nabla \times \mathbf{u}(\mathbf{x}, t)$  represents the only non-zero component of the vorticity field for 2-D flow. Note that the pressure is absent from the formulation. An algorithm that splits the convective-diffusive operator of “Eq. (1)” is employed in accordance with Chorin (1973). The Reynolds number is defined as  $\text{Re} = \frac{U d}{\nu}$ , where  $\nu$  the kinematic viscosity of fluid and  $d$  is the diameter cylinder; the dimensionless time is  $d/U$ . The Vortex Method proceeds by discretizing spatially the vorticity field using a cloud of elemental vortices, which are characterized by a distribution of vorticity,  $\zeta_{\sigma_i}$  (commonly called the cutoff function), the circulation strength  $\Gamma_i$  and the core size  $\sigma_i$ . Thus, the discretized vorticity is expressed by

$$\omega(\mathbf{x}, t) \approx \omega^h(\mathbf{x}, t) = \sum_{i=1}^Z \Gamma_i(t) \zeta_{\sigma_i}(\mathbf{x} - \mathbf{x}_i(t)), \quad (2)$$

where  $Z$  is the number of point vortices of the cloud used to simulate the vorticity field. The numerical analysis is conducted over a series of small discrete time steps  $\Delta t$  for each of which a discrete vortex element  $\Gamma_{(i)}$  is shed from cylinders surfaces. The intensity  $\Gamma_{(i)}$  of these newly generated vortices is determined using the no-slip condition on  $S_1$  and  $S_2$ . NP flat source panels represent cylinders surfaces to ensure impermeability condition on  $S_1$  and  $S_2$  (Katz and Plotkin, 1991). It is assumed that the source strength per length is constant. The velocity field  $\mathbf{u}$  is calculated at the location of elemental vortices in a typical Lagrangian description. The velocity induced by cylinders is calculated in the frame of reference  $(x, o, y)$ , see Moraes (2011). The vortex-vortex interaction is obtained from the vorticity field by means of the Biot-Savart law. The convective motion of each vortex generated on the body surface is determined by integration of each vortex path equation using a first order Euler scheme. The diffusion of vorticity is taken care of using the random walk method (Lewis, 1999).

Starting from the Navier-Stokes equations is obtained a Poisson equation for the pressure. This equation is solved through the following integral formulation (Shintani and Akamatsu, 1994)

$$H \bar{Y}_i - \int_S \bar{Y} \nabla \Xi_i \cdot \mathbf{e}_n dS = \iint_{\Omega} \nabla \Xi_i \cdot (\mathbf{u} \times \boldsymbol{\omega}) d\Omega - \frac{1}{\text{Re}} \int_S (\nabla \Xi_i \times \boldsymbol{\omega}) \cdot \mathbf{e}_n dS, \quad \bar{Y} = p + \frac{u^2}{2}, \quad \mathbf{u} = |\mathbf{u}|, \quad (4)$$

where  $H = 1$  in the fluid domain,  $H = 0.5$  on the boundaries,  $\Xi$  is a fundamental solution of the Laplace equation and  $\mathbf{e}_n$  is the unit vector normal to the cylinders surface,  $S_1$  and  $S_2$ . The drag and lift coefficients are obtained from pressure integration.

### 3. RESULTS AND CONCLUSIONS

The vortex code was validated simulating the flow around an isolated circular cylinder. This was done in order to determine the parameters associated with the numerical method, like: number of flat panels used to represent the circular cylinder (NP=300); position of detachment of the discrete vortices ( $\epsilon_{ps} = 0.0010$ ); Lamb core size ( $\sigma_0 = 0.0010$ ); for more details see Moraes (2011). Each simulation was performed up to 1,600 time steps with a value of  $\Delta t = 0.05$  for dimensionless time step. "Table 1" and "Table 2" present comparisons of present simulation with experimental results from Alam *et al.* (2003). Experiments were conducted in a low-speed, close-circuit wind tunnel with a test section of 0.6 m height, 0.4 m width, and 5.4 m length. The level of turbulence was 0.19%. The geometric blockage ratio and aspect ratio at test section were 8.1% and 8.2%, respectively. The experimental results were not corrected or the effects of wind-tunnel blockage.

Table 5.1 - Comparison between numerical and experimental results for drag coefficient,  $Re = 6,5 \times 10^4$

Case	g/d	Downstream Cylinder		Upstream Cylinder	
		$C_D^+$	$C_D^*$	$C_D^+$	$C_D^*$
1	1,1	1,0953	0,9112	-0,5697	-0,0427
2	1,5	-	0,9095	-0,3884	-0,2683
3	2,0	1,0531	0,8473	-0,2363	-0,4021
4	2,5	-	0,8075	0,0019	-0,2376
5	3,0	0,9866	0,8744	-0,1346	0,2164
6	3,5	0,8912	1,0047	-0,2212	0,5796
7	4,0	0,8800	1,0285	-0,2485	0,5654
8	4,5	1,2612	1,0542	0,2766	0,4937

Table 5.2 - Comparison between numerical and experimental results for Strouhal number,  $Re = 6,5 \times 10^4$

Case	g/d	Downstream Cylinder		Upstream Cylinder	
		$St^+$	$St^* : Q(x,y)$	$St^+$	$St^* : P(x,y)$
1	1,1	0,1365	0,1400	0,1360	0,1400
2	1,5	0,1387	0,1564	0,1365	0,1787
3	2,0	0,1411	0,1333	0,1411	0,1282
4	2,5	0,1387	0,1800	0,1411	0,1800
5	3,0	0,1365	0,1600	0,1387	0,2000
6	3,5	0,1350	0,1800	0,1365	0,1800
7	4,0	0,1818	0,1800	0,1818	0,1800
8	4,5	0,1867	0,2000	-	0,2000

<sup>+</sup> Experimental results (Alam *et al.*, 2003)

<sup>\*</sup> Present Simulation

The experimental results revealed a discontinuous jump on drag coefficient and Strouhal number at critical spacing gap  $g/d=4$ . The discontinuity was interpreted as the result of an abrupt change from one stable flow pattern to another; this behaviour was classified as bi-stable state. On the other hand, the numerical results revealed the discontinuous

jump at  $g/d=3$ . The results from Biermann and Herrstein (1933), showed the bi-stable state on time-averaged drag coefficient for downstream cylinder at  $g/d \approx 3$  in agreement with the present numerical results.

When the spacing between cylinders is larger than the critical spacing, the flow pattern is referred as co-shedding type. Figure 2 shows the possible binary-vortex structure for spacing gap  $g/d=4.5$ , with both cylinders shedding vortices. The main purpose of this work was to identify a possible formation of a binary vortex street behind downstream cylinder (Zdravkovich, 1987). The vortex formation from two cylinders is independent for  $g/d > 6-8$ .



Figure 2. Position of the binary-vortex street at  $t=75$  for the spacing gap  $g/d=4.5$ .

Computed values for time-evolution drag and lift coefficients are plotted in Fig. 3. Figure 4 shows plots of instantaneous pressure distributions on the cylinders surface for the spacing gap  $g/d=4.5$ . Pressure distributions A, B, C, D and E are related to instants A, B, C, D and E as indicated in Fig. 3. The vortex shedding effect can be seen in oscillations of the lift and drag coefficients. As soon as the numerical transient is over and the periodic steady state regime is reached (from  $t = 22$  on, approximately) the upstream cylinder lift coefficient shows a mean variation between  $-1.19$  and  $1.12$ , approximately, with a dimensionless frequency (Strouhal number) about twice the frequency of the drag coefficient, in accordance to the physics involved in the flow. Figure 3(a) indicates that the fluctuation of  $C_D$  has twice the frequency of  $C_L$ , because it fluctuates once for each of upper and lower shedding.

The time history of drag and lift curves for downstream cylinder present interference effects due to the upstream cylinder viscous wake; see in Fig. 3(b).

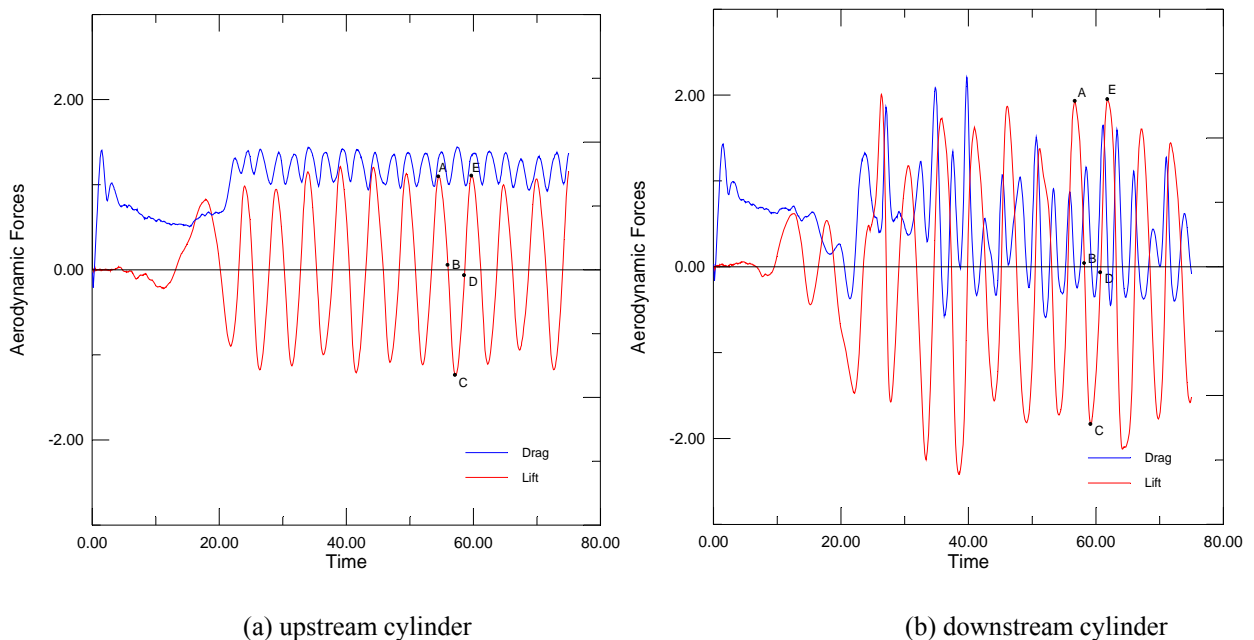
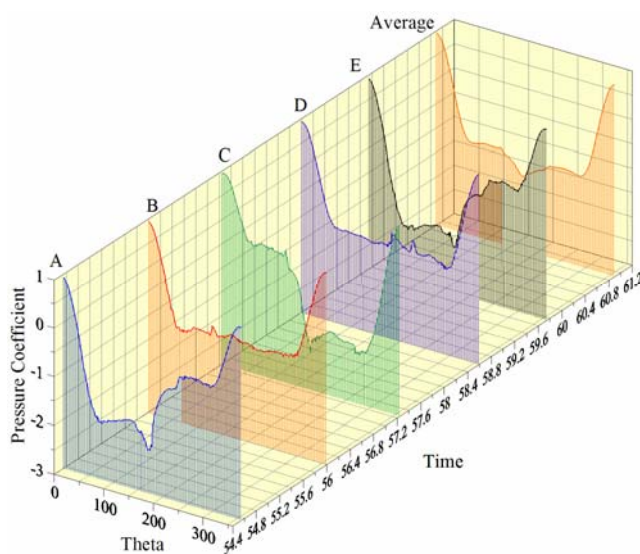
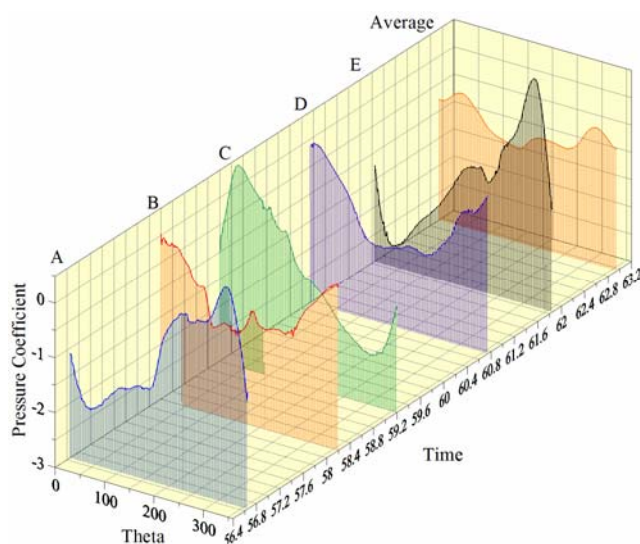


Figure 3. Time history of drag and lift coefficients for two circular cylinders in tandem arrangement for the spacing gap  $g/d=4.5$ .

For both Fig 3(a) and Fig 3(b) the instant A is defined by a maximum value of the lift coefficient; at this moment a large clockwise vortex structure (in fact a cluster of vortices) is detaching from the upstream circular cylinder upper surface and moving toward the binary vortex-street; this structure is indicated in Fig. 5(a). As this structure moves downstream it pushes away an anti-clockwise structure that was stationed behind the upstream cylinder and the drag coefficient increases. At instant B the anti-clockwise structure detaches from the upstream cylinder surface and is incorporated into the viscous wake; this process creates a low pressure region at the rear part of the upstream cylinder which is associated to the high drag value (Fig. 3 and Fig. 4). At this moment a new anti-clockwise vortex structure that has already started at the low side of the upstream cylinder surface can be observed. The above described sequence of events repeats all over again. Therefore, the lowest value of the lift coefficient is observed when another cluster, now rotating in the anti-clockwise direction, leaves the upstream body surface (point C in Fig. 4(a) and Fig. 5(c)).



(a) upstream cylinder



(b) downstream cylinder

Figure 4. Instantaneous pressure distributions for two circular cylinders in tandem arrangement for the spacing gap  $g/d=4.5$ .

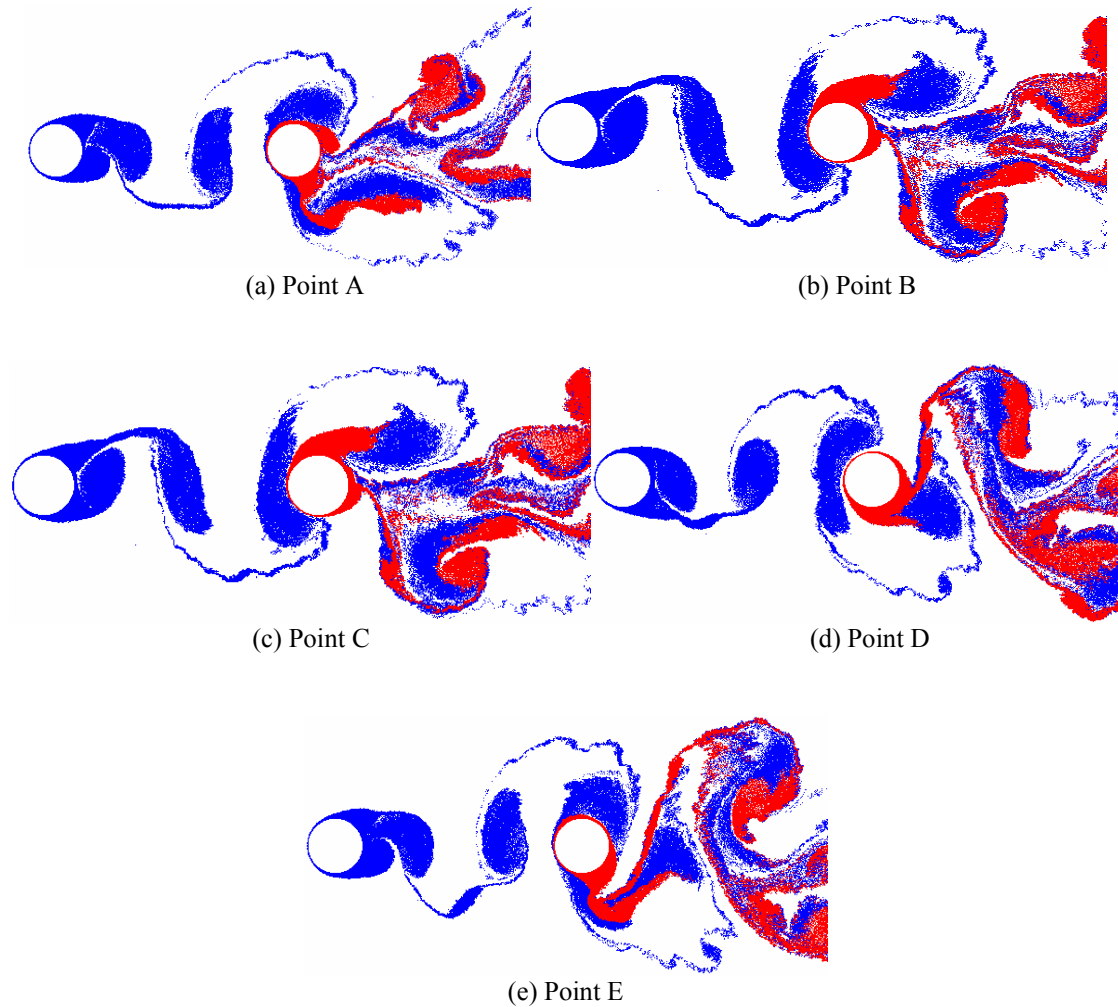


Figure 5. Near wake behaviour between  $t=56.65$  and  $t=61.85$  for two circular cylinders in tandem arrangement for the spacing gap  $g/d=4.5$ .

There are many unknown and discrepant points in previous studies on two immovable circular cylinders arranged in tandem (Igarashi, 1981). In the literature, there have been very few studies by considering measure of fluctuating lift and drag forces on the cylinders. Therefore, the present numerical study was motivated by both fundamental and practical considerations.

As future work, a tandem pair of cylinders with downstream one free to oscillate will be investigated. The analysis will evolve: dynamic responses in amplitude and dominant oscillation frequency; instantaneous phase angle between fluid forces and cylinder displacement and phase angle between the immovable upstream cylinder and downstream cylinder oscillations.

#### 4. ACKNOWLEDGEMENTS

This work was supported by FAPEMIG (Proc. TEC-APQ-01070-10 and Proc. PCE-00551-12).

#### 5. REFERENCES

- Alam, M.M., Moriya, M., Takay, K. and Sakamoto, H., 2003, "Fluctuating Fluid Forces Acting on Two Circular Cylinders in a Tandem Arrangement at a Subcritical Reynolds Number", *Journal of Wind Engineering and Industrial Aerodynamics*, Vol. 91, pp. 139-154.
- Bierman, D. and Herrnstein, J., 1933, "The Interference between Struts in Various Combinations", National Advisory Committee for Aeronautics, Technical Report 468.
- Carmo, B.S., Meneghini, J.R. and Sherwin, S.J., 2010a, "Possible States in the Flow around Two Circular Cylinders in Tandem with Separation in the Vicinity of the Drag Inversion Spacing", *Physics of Fluids*, Vol. 22, 054101.
- Carmo, B.S., Meneghini, J.R. and Sherwin, S.J., 2010b, "Secondary Instabilities in the Flow around Two Circular Cylinders in Tandem", *Journal of Fluid Mechanics*, Vol. 644, pp. 395-431.

- Chorin, A.J., 1973, "Numerical Study of Slightly Viscous Flow", *Journal of Fluid Mechanics*, Vol. 57, pp. 785-796.
- Igarashi, T., 1984, "Characteristics of the Flow around Two Circular Cylinders Arranged in Tandem (second report, unique flow phenomenon at small spacing)", *Bulletin of the JSME*, Vol. 27, pp. 2380-2387.
- Igarashi, T., 1981, "Characteristics of the Flow around Two Circular Cylinders Arranged in Tandem (first report)", *Bulletin of the JSME*, Vol. 24, pp. 323-331.
- Katz, J. and Plotkin, A., 1991, "Low Speed Aerodynamics: From Wing Theory to Panel Methods". McGraw Hill, Inc.
- Lewis, R.I., 1999, "Vortex Element Methods, the Most Natural Approach to Flow Simulation - A Review of Methodology with Applications", *Proceedings of 1<sup>st</sup> Int. Conference on Vortex Methods*, Kobe, Nov. 4-5, pp. 1-15.
- Moraes, P.G., 2011, "Efeitos de Interferência entre Dois Corpos Idênticos Alinhados com o escoamento", M.Sc. Dissertation, Mechanical Engineering Institute, UNIFEI, Itajubá, MG, Brazil (in Portuguese).
- Shintani, M. and Akamatsu, T., 1994, "Investigation of Two Dimensional Discrete Vortex Method with Viscous Diffusion Model", *Computational Fluid Dynamics Journal*, Vol. 3, No. 2, pp. 237-254.
- Sumner, D., 2010, "Two Circular Cylinders in Cross-Flow: A Review", *Journal of Fluid and Structures*, Vol. 26, pp. 849-899.
- Xu, G. and Zhou, Y., 2004, "Strouhal Numbers in the Wake of Two Inline Cylinders", *Experiments in Fluids*, Vol. 37, pp. 248-256.
- Zdravkovich, M.M., 1987, "The Effects of Interference between Circular Cylinders in Cross Flow", *Journal of Fluid and Structures*, Vol. 1, pp. 239-261.
- Zdravkovich, M.M., 1977, "Review of Flow Interference between Two Circular Cylinders in Various Arrangements", *ASME Journal of Fluid Engineering*, Vol. 99, pp. 618-633.
- Zhou, Y. and Yiu, M.W., 2006, "Flow Structure, Momentum and Heat Transport in a Two-Tandem-Cylinder Wake", *Journal of Fluid Mechanics*, Vol. 548, pp. 17-48.

## 6. RESPONSIBILITY NOTICE

The authors are the only responsible for the printed material included in this paper.